HJPED

HJ

Article

Assessing Climate-Based Tourism Suitability in Nigeria (1991–2024) Using the Tourism Climate Index and TerraClimate Dataset.

Academic Editor: Prof. Azizur Rahaman

Received: 10.11.2025
Revised: 10.01.2026
Accepted: 12.01.2026
Published: 15.01.2026

Ugo Uwadiako Enebeli[1], Rejoice Kaka Hassan[2], Yakubu Joel Cherima[2], Fiyidi Mikailu[3], Yonwul Jacqueline Dakyen[4], Kebiru Umoru[5] and Zubairul Islam[5], Ebelechukwu Lawrence Enebeli[6]

[1]Department of Community Medicine, Rhema University, Aba, Abia State, Nigeria;
ugoenebeli@rhemauniversity.edu.ng (U.U.E.), https://orcid.org/0000-0001-5950-3719
[2]Department of Policy and Strategic Studies, University of Abuja, Federal Capital Territory, Nigeria;
ycherima@gmail.com (Y.J.C.) https://orcid.org/0009-0004-3724-9886;
rejoice.diara@gmail.com (R.K.H.) https://orcid.org/0009-0007-1269-0546
[3]Young Individual Development Initiative, Nigeria;
fiyidimi@gmail.com (F.M.), ORCID ID: 0009-0002-4804-8794
[4]Independent Public health Researcher, Nigeria;
ydakyen@yahoo.com (Y.J.D.), https://orcid.org/0009-0006-7229-4943
[5]Faculty of Environmental Sciences (FES), Hensard University, Bayelsa 56110, Nigeria;
zubairul@gmail.com (Z.I.), https://doi.org/10.1080/23729333.2023.2298525, kabiirchief@yahoo.com (KU).
[6]Department of Science and Technology, Lancaster University, Accra, Ghana;
eby.enebeli@gmail.com (E.L.E), https://orcid.org/0009-0007-8434-5485

*Correspondence: ugoenebeli@rhemauniversity.edu.ng

Abstract

Tourism and outdoor recreation in Nigeria are tightly coupled to meteorological conditions that vary sharply across latitude, seasons, and terrain. We develop a nation-scale, monthly assessment of climate suitability for tourism for 1991–2024 by deriving intermediate meteorological metrics and composite indices from TerraClimate (~4.6-km) and assembling the Tourism Climate Index (TCI) via Temperature–Humidity Index (THI)–based daytime (CID) and 24-h (CIA) comfort components. Inputs (tmmx, tmmn, pr, srad, vap, vs) were scaled and stacked in Google Earth Engine; astronomical radiation terms (Ra, daylength) and sunshine hours (Ångström–Prescott) were computed in R (terra). Outputs comprise harmonized rasters and area-weighted summaries for all 36 states and the Federal Capital Territory using OSGOF ADM1 boundaries. Results reveal a coherent, process-based geography. The semi-arid north achieves the highest mean TCI—e.g., Yobe 84.55, Sokoto 83.90, Jigawa 82.57, Gombe 82.41, Adamawa 82.19, Kebbi 82.35, Kano 82.12—driven by more frequent sunshine (S) and lower precipitation penalties (R), with CID/CIA near the comfort pivot. Humid coastal states score lower primarily due to persistent cloud/rain and high vapor pressure that elevates THI (e.g., Rivers 70.60, Bayelsa 70.92, Akwa Ibom 71.75, Delta 72.32, Abia 73.03, Lagos 74.61). State-level standard deviations are modest (~1.1–3.1 TCI units), but wide p10–p90 gaps along the coast indicate strong monsoonal seasonality; northern states show tighter intra-annual ranges. Orographic and ecotonal states (Plateau, Taraba) exhibit the broadest dispersion, reflecting elevation-controlled thermal and cloud variability. Methodologically, the pipeline is transparent and reproducible, linking remote-sensing–compatible inputs to policy-facing summaries. Practical implications include calendar-aware event scheduling, destination portfolio shifts by season, and integration of TCI calendars with health/safety protocols for heat and heavy rainfall. Limitations—THI as a proxy for effective temperature, generic Ångström–Prescott coefficients, ~4-km grid resolution, and ADM1 aggregation motivate sensitivity tests (e.g., PET/UTCI substitution, local sunshine calibration) and finer operational products. This work provides climate-comfort baseline to support tourism planning and climate-risk management.

Keywords: Tourism Climate Index (TCI), Temperature–Humidity Index (THI), TerraClimate.

1. Introduction

Nigeria's climate shapes mobility, productivity, and public well-being for over 200 million people across coastal megacities and expanding inland hubs (Niang et al., 2014; World Bank, 2023). Tourism, outdoor recreation, and service economies are particularly sensitive to heat, humidity, wind, rainfall, and sunshine—drivers that also modulate health risks, energy demand, and transport reliability (Scott & Lemieux, 2010; de Freitas et al., 2017). The country's seasonal contrasts between the humid south and the semi-arid north, coupled with the Harmattan period, create pronounced swings in thermal comfort and sky conditions that are consequential for event planning, leisure, and urban amenity design (Odjugo, 2011; Oguntunde et al., 2017).

Despite a growing literature on climate–tourism linkages in tropical and Mediterranean contexts, decision-ready metrics translating meteorology into human-perceived comfort remain under-represented in Nigerian policy and market analytics (Amelung et al., 2007; Perch-Nielsen et al., 2010). To address this gap, we develop a nation-scale, monthly assessment of climate suitability for tourism and outdoor activities in Nigeria by deriving intermediate meteorological metrics and composite tourism indices from the TerraClimate dataset (Abatzoglou et al., 2018). Specifically, we compute temperature means, radiation and sunshine diagnostics, humidity measures, wind, and precipitation; transform these to Temperature–Humidity Index (THI) for both daytime and 24-hour comfort; and aggregate them into Mieczkowski's Tourism Climate Index (TCI) (Mieczkowski, 1985; de Freitas et al., 2017).

Outputs are produced as harmonized rasters and summarized at the state (ADM1) level to support benchmarking, seasonal calendars, and spatial comparison across Nigeria's ecological and socio-economic zones. Given the pace of urbanization and infrastructure growth, climate comfort has become an actionable constraint for planners, investors, and destination managers (Gössling et al., 2012). Heat-stress episodes and humidity spikes reduce outdoor dwell times, shift demand toward climate-controlled venues, and depress open-air commerce; conversely, windows of favorable sunshine and moderate wind can be leveraged for festivals, coastal visitation, and ecotourism (Scott et al., 2019). Establishing a spatially resolved, reproducible climate-comfort baseline—linked to remote-sensing-compatible datasets—therefore provides a practical foundation for tourism scheduling, marketing, and climate-risk reduction in Nigeria.

To the best of our knowledge, there is no long, consistent, sub-national analysis that (i) converts multi-decadal, gridded climate data into interpretable thermal-comfort metrics, (ii) maps monthly tourism suitability across Nigeria's states, and (iii) quantifies spatial–seasonal contrasts with reproducible workflows. We therefore ask: (1) How do THI-based thermal comfort and TCI vary across Nigeria's climatic zones and seasons (1991–2024)? (2) Which components—rainfall, sunshine, wind, or humidity—most strongly limit or enable favorable conditions in different regions? (3) How can state-level summaries and maps inform practical calendars for tourism and outdoor programming?

Methodologically, we provide an open, end-to-end pipeline that transforms TerraClimate inputs into THI/TCI layers using FAO-56 formulations and Mieczkowski's structure, delivering state-level statistics suitable for dashboards and planning. Substantively, we furnish a multi-decadal, spatially explicit picture of Nigeria's climate comfort, identifying high-opportunity months and locations as well as constraint drivers. Practically, the outputs support data-driven scheduling (events, holidays, site visits), portfolio diversification across states, and climate-aware destination management. Together, these contributions advance the operational use of climate information in Nigeria's tourism and outdoor-economy strategy.

2. Materials and methods

2.1. Study Area

This study covers the Federal Republic of Nigeria (≈ 4°–14° N, 3°–14° E), comprising 36 states and the Federal Capital Territory (FCT). Nigeria extends over ~924,000 km² from the Atlantic coastline of the Gulf of Guinea in the south through the humid forest belt and Guinea savannas to the Sudano–Sahelian zone bordering Niger and Chad (Adefisan & Abatan, 2020; Oladipo, 1995). Relief ranges from coastal lowlands and the Niger–Benue trough to elevated uplands, including the Jos Plateau (~1,200–1,400 m) and Mambilla Plateau, which generate strong meso-climatic contrasts (Balogun et al., 2016; Ayuba et al., 2018).

Nigeria's population exceeds 200 million, concentrated in major urban centers such as Lagos, Abuja, Kano, Port Harcourt, Ibadan, and Kaduna, where outdoor economy and tourism activities are highly climate-sensitive (UNDESA, 2023; NBS, 2022).

Climatologically, the south experiences a humid monsoonal regime with long wet seasons and persistent high humidity, transitioning northward to a single-peak rainy season and increasing aridity (Tsanakas et al., 2019). The Harmattan period (boreal winter) introduces dry, dusty northeasterlies that depress humidity, reduce visibility, and markedly alter thermal comfort and sky clarity (Adedokun, 1978; Omotosho, 2008).

For spatial analysis, we used OSGOF (2019) ADM1 boundaries for all state-level reporting. Gridded outputs were clipped to national land boundaries (excluding offshore pixels) and aggregated to the state/FCT level. This latitudinal gradient, coupled with coastal exposure, complex topography, and dense urban clusters, establishes a natural laboratory for assessing Temperature–Humidity Index (THI) and Tourism Climate Index (TCI) variability across ecological and administrative zones (Akinsanola et al., 2017; Olaniran et al., 2020).

.

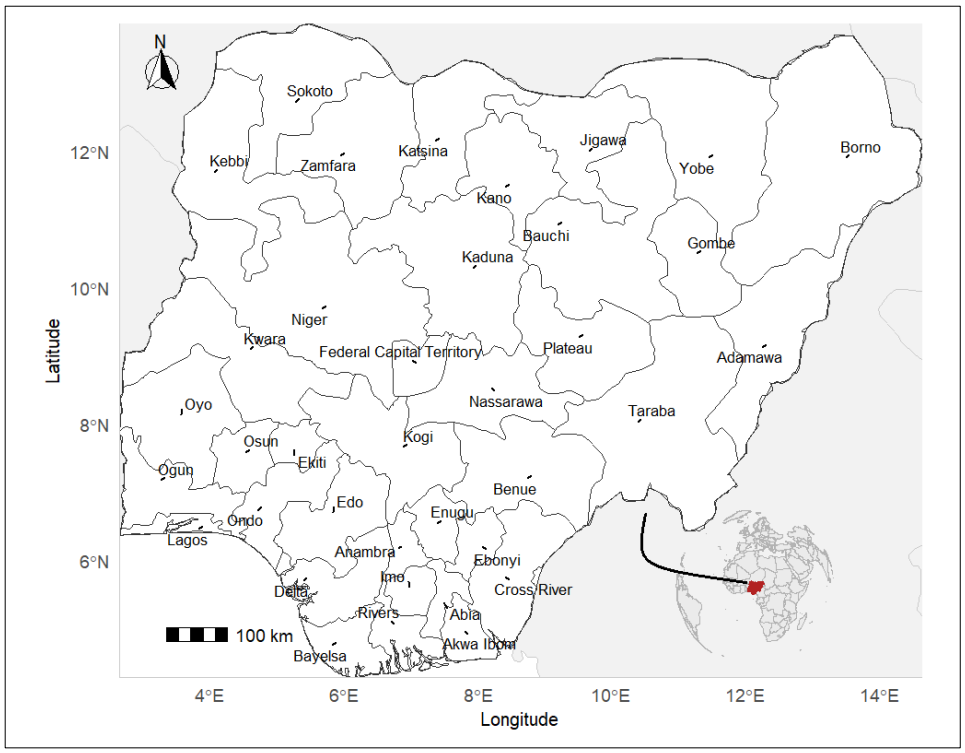

Figure 1 Location of Nigeria.

2.3 Schematic Workflow

TerraClimate inputs are scaled and stacked in Google Earth Engine, intermediate radiative/astronomical and humidity variables are computed in R (FAO-56; Ångström–Prescott), thermal

comfort (THI) is mapped to CID/CIA, precipitation/sunshine/wind sub-indices (R, S, W) are scored, and the Tourism Climate Index (TCI) is assembled and bounded. Outputs include monthly rasters, state-level (ADM1) statistics via area-weighted aggregation, and publication-ready maps and tables.

2.2 Data Sources and Processing

Table 2. Derived climate metrics and tourism indices computed from TerraClimate inputs.

Layer	Built from	Method (key formula)	Units
Tmean	Tmax, Tmin	Tmean=(Tmax+Tmin)/2	°C
Daily global radiation (Rs)	SRAD	Rs=SRAD×0.0864	MJ·m^{-2}·day^{-1}
Extraterrestrial radiation (Ra)	Lat, DOY	FAO-56	MJ·m^{-2}·day^{-1}
Daylength (N)	Lat, DOY	N=24/π W_s	hours·day^{-1}
Sunshine hours (SunH)	Rs, Ra	Ångström–Prescott	hours·day^{-1}
RHmin, RHmean	VAP, Tmax/Tmean	FAO-56	%
THI (day/mean)	T, RH	THI=T−0.55(1−RH/100)(T−14.5)	index
CID, CIA	THI(day/mean)	THI mapped to Mieczkowski's [−3,5]	score (−3…5)
R, S, W (TCI sub-indices)	PPT, SunH, WS	Mieczkowski's discrete bins (PPT in mm·month^{-1}; SunH in h·day^{-1}; WS in m·s^{-1})	score (0…5)
TCI	CID, CIA, R, S, W	TCI=2 (4 CID+CIA+2R+2S+W), bounded to [0,100]	0–100

2.2.1 Climate data and preprocessing

We used TerraClimate monthly grids (ID: IDAHO_EPSCOR/TERRACLIMATE) for 1991–2024 at ~4.6-km native resolution (Abatzoglou et al., 2018). The following variables were exported: monthly maximum and minimum air temperature (tmmx, tmmn), precipitation (pr), surface downwelling shortwave radiation (srad), vapor pressure (vap), and 10-m wind speed (vs). In Earth Engine we applied the official scale factors prior to export: tmmx/tmmn ×0.1 (°C), srad ×0.1 (W m^{-2}), vap ×0.001 (kPa), vs ×0.01 (m s^{-1}), while precipitation is in mm month^{-1}. Per variable, monthly images were stacked into a multiband GeoTIFF at 4,000-m pixel size (Web Mercator, EPSG:3857) (Gorelick et al., 2017; Funk et al., 2015).

2.2.2 Derivation of intermediate climate metrics (R)

All subsequent processing was conducted in R using the terra package. For astronomical terms we built a latitude raster in degrees by projecting a reference layer to geographic coordinates (EPSG:4326) and reprojecting the latitude grid back to the analysis grid to avoid projection artifacts. From TerraClimate radiation we computed daily global radiation Rs as Rs=srad×0.0864 (MJ m^{-2} d^{-1}). Extraterrestrial radiation Ra (MJ m^{-2} d^{-1}) and daylength N (h) were obtained following FAO-56 (Allen et al., 1998):

$$d_r = 1 + 0.033cos\left(\frac{2\pi J}{365}\right), \delta = 0.409sin\left(\frac{2\pi J}{365} - 1.39\right), w_s = arccos(-tan\emptyset tan\vartheta), \quad (1)$$

$$R_a = \frac{20.60}{\pi} G_{SC} d_r [sinw_s\, cos\emptyset cos\delta + w_s sin\emptyset sin\delta], N = \frac{24}{\pi} w_s, \quad (2)$$

with Gsc=0.0820 MJ m^{-2} min^{-1}, latitude ϕ in radians, and day-of-year J (Allen et al., 1998; Hargreaves & Samani, 1985). Sunshine hours were estimated via Ångström–Prescott using default coefficients a=0.25, b=0.50:

$$\frac{n}{N} = \frac{{}^{R_s}/_{R_a} - a}{b}, SunH = n = \frac{{}^{R_s}/_{R_a} - a}{b} N, 0 \le \frac{n}{N} \le 1. \quad (3)$$

Saturation vapor pressure followed FAO-56(T) =0.6108 $\exp\left(\frac{17.2T}{T+237.3}\right)$(kPa). We then derived RH_{min}=(vap/$e_s(T_{max})$)×100 and H_{min}=(vap/$e_s(T_{mean})$)×100 (clamped 1–100%).

2.2.3 Tourism Climate Index (TCI)

The Tourism Climate Index (TCI) was computed following Mieczkowski's structure (Mieczkowski, 1985; Amelung et al., 2007):

$$TCI = 2(4CID + CIA + 2R + 2S + W), \quad (4)$$

where CID and CIA are thermal comfort ratings for daytime and 24-h periods, R is precipitation, S sunshine, and W wind, each on Mieczkowski's discrete scales (de Freitas et al., 2017; Mora et al., 2017). Because the original CID/CIA charts are based on effective temperature tables, we used a standard Temperature–Humidity Index (THI) proxy,

$$THI = T - 0.55(1 - RH/100)(T - 14.5), \quad (5)$$

mapping THI to the [−3,5] CID/CIA categories consistent with the comfort ranges reported by Mieczkowski (optima ~20–27 °C; slightly warmer tolerance for daytime). R, S, and W were scored using the original TCI bin thresholds (mm $month^{-1}$; sunshine h d^{-1}; m s^{-1}). Final TCI values were bounded to [0,100] (Scott et al., 2016; Rutty & Scott, 2010).

.

2.2.4 Spatial aggregation and reporting

Raster summaries were produced at the state (ADM1) level using the official OSGOF 2019 boundary file. To account for partial pixel coverage, we computed area-weighted statistics by extracting all cell values intersecting each polygon along with fractional overlap weights and then calculating weighted mean, median, standard deviation, minima, maxima, and 10th/90th percentiles in R. For national reference, unmasked raster means were also reported. All maps are shown for monthly fields in 2024 and their 2024 annual means; long-term (1991–2024) means were used where explicitly stated.

2.2.5 Software & reproducibility

Data acquisition and export were performed in Google Earth Engine (script provided), while all transformations and indices were computed in R (terra). Dataset provenance and variable definitions follow TerraClimate documentation; astronomical and humidity formulations follow FAO-56; TCI construction follows Mieczkowski (1985).

3. Results

3.1. Spatiotemporal Trends in Environmental Indicators (1991–2023)

Thermal gradients (Tmax, Tmin).

A clear north–south temperature gradient emerges. Coastal and forest states cluster at lower Tmax (e.g., Lagos mean 31.81 °C; Bayelsa 31.97 °C; Akwa Ibom 32.32 °C), while the Sudano–Sahelian belt peaks near 35–36 °C (e.g., Borno 35.80 °C, Sokoto 35.65 °C, Jigawa 35.22 °C). Medians track means closely (typical sd ≈ 0.2–0.9 °C), indicating stable monthly central tendencies. Nighttime Tmin shows the inverse pattern—warmer along the coast (e.g., Lagos 24.84 °C, Rivers 24.01 °C) and coolest on the central/northern highlands and plains (≈ 19–22 °C in Jigawa, Kano,

Kaduna). Orographic states exhibit wider spread: Plateau shows the largest temperature variability (Tmax sd 2.61 °C; Tmin sd 2.48 °C), consistent with elevation and complex relief.

Hydro-radiative controls (PPT, SRAD).

Moisture supply is highest in the Niger Delta and coastal southeast (e.g., Bayelsa mean PPT ≈ 253 mm month^{-1}; Rivers 217 mm; Delta 201 mm), and lowest in the interior north/central corridor (e.g., Kwara 62 mm; Jigawa 67 mm; Yobe 67 mm), with several states showing wide p10–p90 spans (> 40 mm), reflecting strong seasonal cycling. By contrast, mean shortwave radiation (SRAD) increases poleward and inland, peaking in the north (e.g., Borno 233 W m^{-2}; Yobe 227 W m^{-2}; Sokoto 226 W m^{-2}) and easing along the cloudier coast (~185–195 W m^{-2} in Rivers, Akwa Ibom, Lagos). This anti-phase of PPT and SRAD is consistent with monsoonal cloudiness and establishes the radiative backdrop for tourism sunlight (S) scoring.

Moisture and thermal stress (VAP).

Near-surface vapor pressure (VAP) mirrors the humidity gradient: highest along the Gulf of Guinea (≈ 3.1 kPa in Lagos, Rivers, Akwa Ibom) and lowest in northern states (≈ 1.75–1.95 kPa in Jigawa, Yobe, Borno). Combined with Tmax/Tmin, these contrasts imply higher THI (greater sultriness) in the south despite milder air temperatures, and lower THI (drier heat) in the north—key for the CID/CIA components of TCI.

Wind environment (WS).

Monthly mean 10-m wind speeds are modest nationwide but systematically higher in the northern belt (e.g., Katsina 2.75 m s^{-1}; Sokoto 2.74 m s^{-1}; Kano 2.55 m s^{-1}) and lighter across the southeast (≈ 1.42–1.56 m s^{-1} in Anambra, Ebonyi, Imo). Lagos stands out among coastal states with relatively brisk winds (2.32 m s^{-1}), potentially offsetting humidity during favorable months. These patterns translate into higher W-subindex scores in the north and lower scores in calmer, humid southern interiors.

Spatial heterogeneity and implications.

States with complex terrain (Plateau, Taraba) show the widest p10–p90 envelopes and standard deviations across variables, underscoring altitude and topographic controls on local climate. Most states exhibit small mean–median offsets, indicating limited skew at the monthly scale, while coastal states pair high PPT with lower SRAD and high VAP (comfort penalty from rainfall/humidity), and northern states pair high SRAD and WS with low PPT/VAP (comfort penalty from hot, dry conditions). Together, these gradients clarify the drivers behind Figure 3's spatial patterns and foreshadow seasonal windows in which different regions of Nigeria achieve favorable combinations for tourism and outdoor activities.

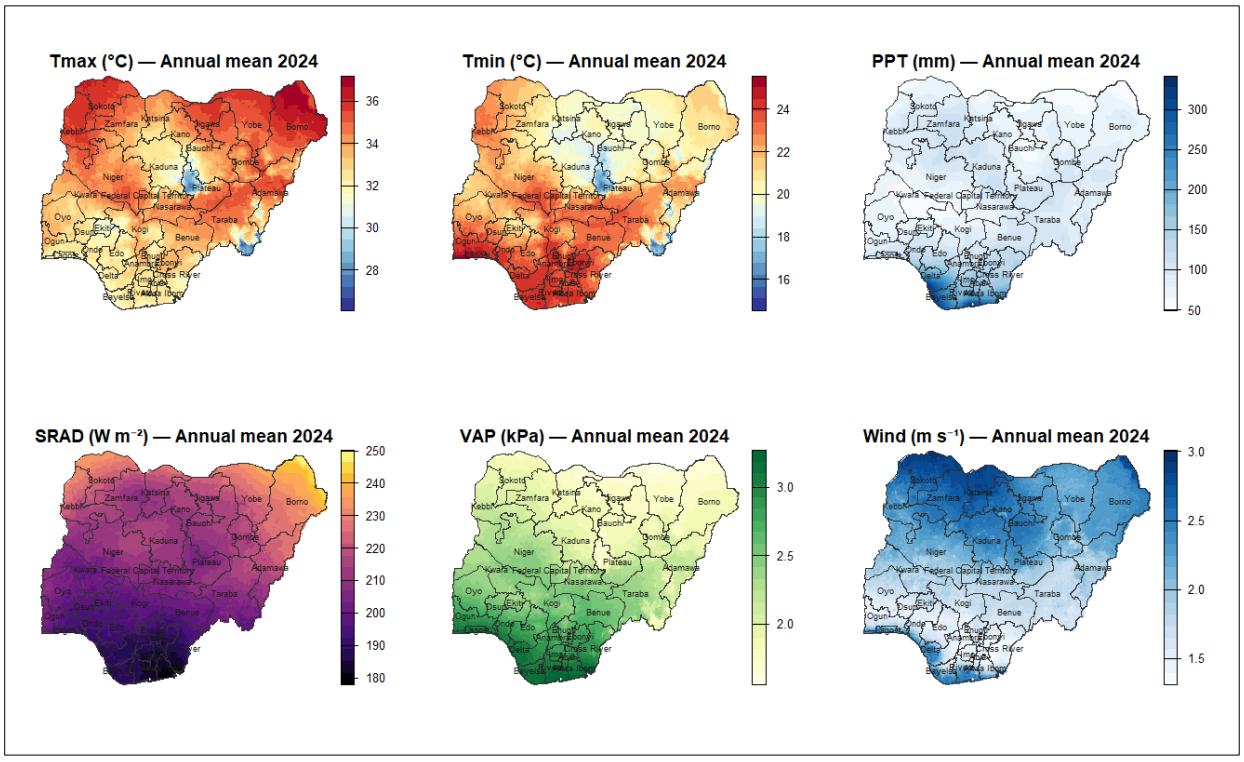

Figure 2. Spatial distribution of annual mean climate variables across Nigeria for 2024.

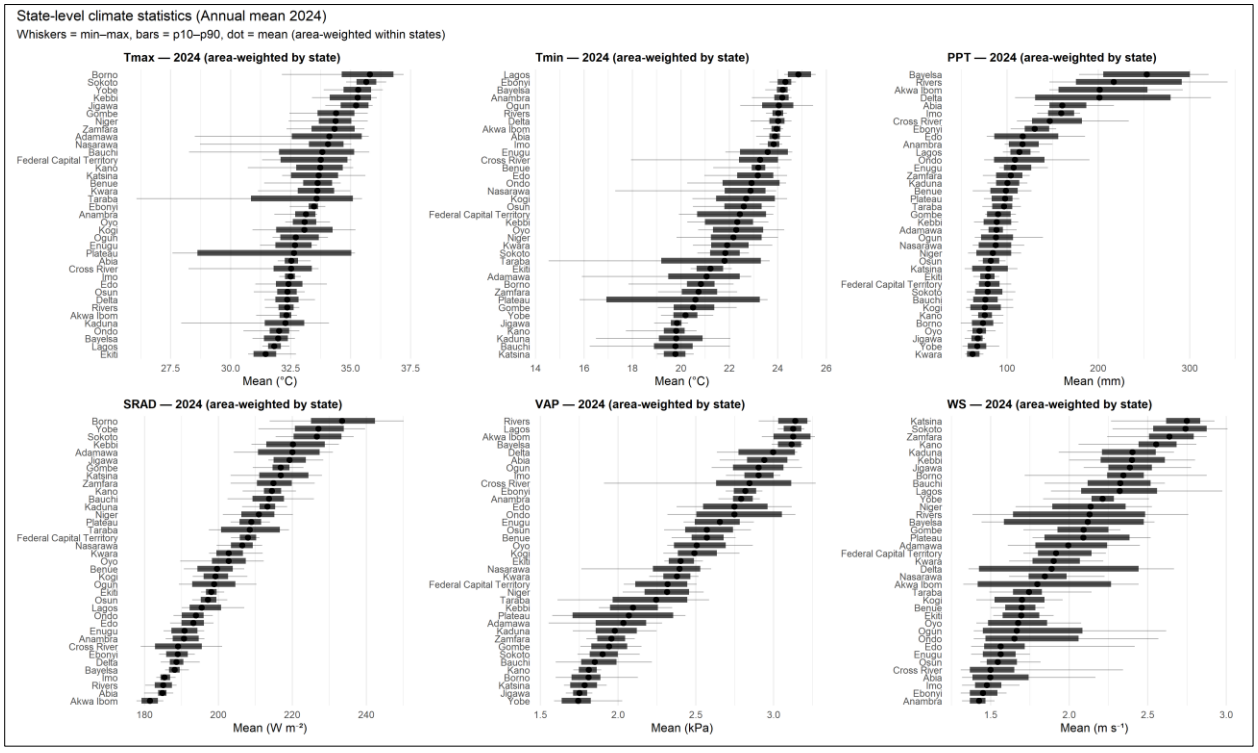

Figure 3. State-level climate statistics for Nigeria (annual means, 2024).

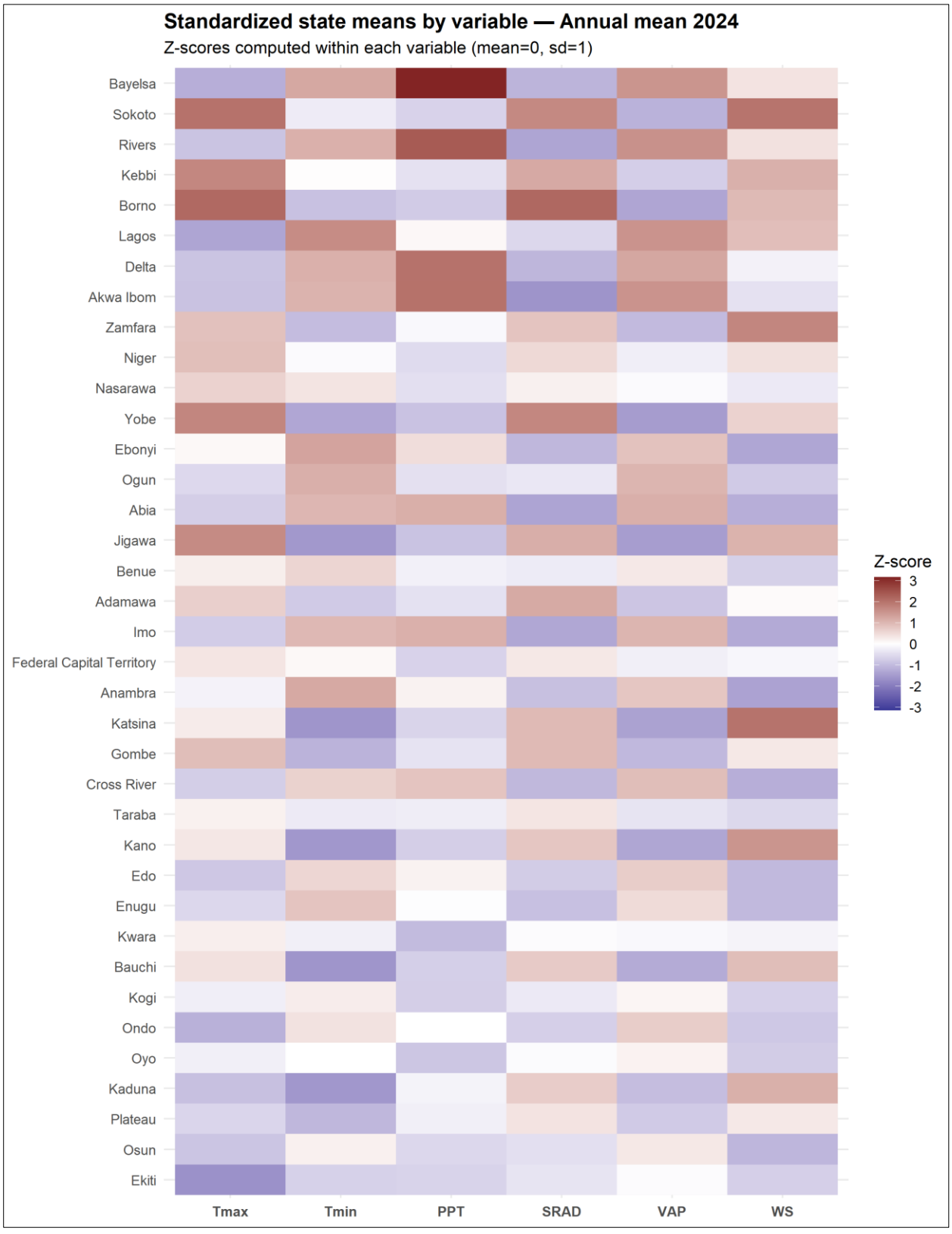

Figure 4. Standardized state-level climate means across Nigeria for 2024.

3.2 Indexes

Thermal comfort (CID, CIA).

Daytime (CID) and 24-h (CIA) comfort scores cluster around 4.7–5.0 (median) nationwide, with north-eastern and north-western states showing higher upper tails in hot, dry months (e.g., Borno CID mean 5.62, Sokoto 5.70; Yobe CIA mean 5.12). Humid coastal states remain close to the comfort pivot but with slightly lower medians (e.g., Rivers CIA median 4.58; Delta 4.58). Orographic and ecotonal settings exhibit broader dispersion—e.g., Taraba and Plateau—consistent with intra-state thermal heterogeneity.

Precipitation penalty/benefit (R).

The R sub-index separates drier interior states (higher R scores; e.g., Sokoto mean 3.95; Kano 4.67; Bauchi 4.30) from wetter coastal belts (lower medians; e.g., Rivers median 1.88; Bayelsa 1.67; Akwa Ibom 1.88). Large p10–p90 spans in many southern states (e.g., Delta, Edo, Ogun) reflect strong monsoonal seasonality—months with very low scores during peak rains contrasted with moderate scores in the dry season.

Sunshine availability (S).

Sunshine scores rise northward, tracking the SRAD gradient: Jigawa (S mean 3.26), Katsina (3.20), Yobe (3.52) and Sokoto (3.53) outperform humid coastal states such as Abia (2.08), Akwa Ibom (2.02) and Rivers (2.14). Medians confirm this pattern (north ≈3.1–3.3 vs. south ≈2.0–2.4), indicating more frequent clear-sky conditions inland.

Wind environment (W).

Most states sit in the "moderate–favorable" band (≈3.6–4.3). Coastal-inland south often attains higher W scores (≈4.1–4.3; e.g., Abia, Enugu, Ebonyi) despite lower absolute wind speeds, likely reflecting the TCI preference for moderate winds. Northern states commonly score 3.5–3.9 (e.g., Kano 3.60; Sokoto 3.55), suggesting occasional winds exceed the comfort optimum even as they aid thermal relief.

Composite Tourism Climate Index (TCI).

The highest TCI means concentrate in the semi-arid north—Yobe 84.55, Sokoto 83.90, Jigawa 82.57, Gombe 82.41, Adamawa 82.19, Kebbi 82.35, Kano 82.12—driven by high S and favorable R, with CID/CIA near comfort. Lower TCI appears across humid coastal states where rainfall and cloudiness suppress scores: Rivers 70.60, Bayelsa 70.92, Akwa Ibom 71.75, Delta 72.32, Abia 73.03, Lagos 74.61. Inland southwest and central states are intermediate to high (e.g., Ekiti 81.07; Kwara 81.25; Niger 80.83). Standard deviations are modest (≈1.1–3.1), but p10–p90 gaps underscore strong seasonality, with coastal states showing the widest intra-annual swings due to the monsoon, and northern states exhibiting more consistently favorable months.

.

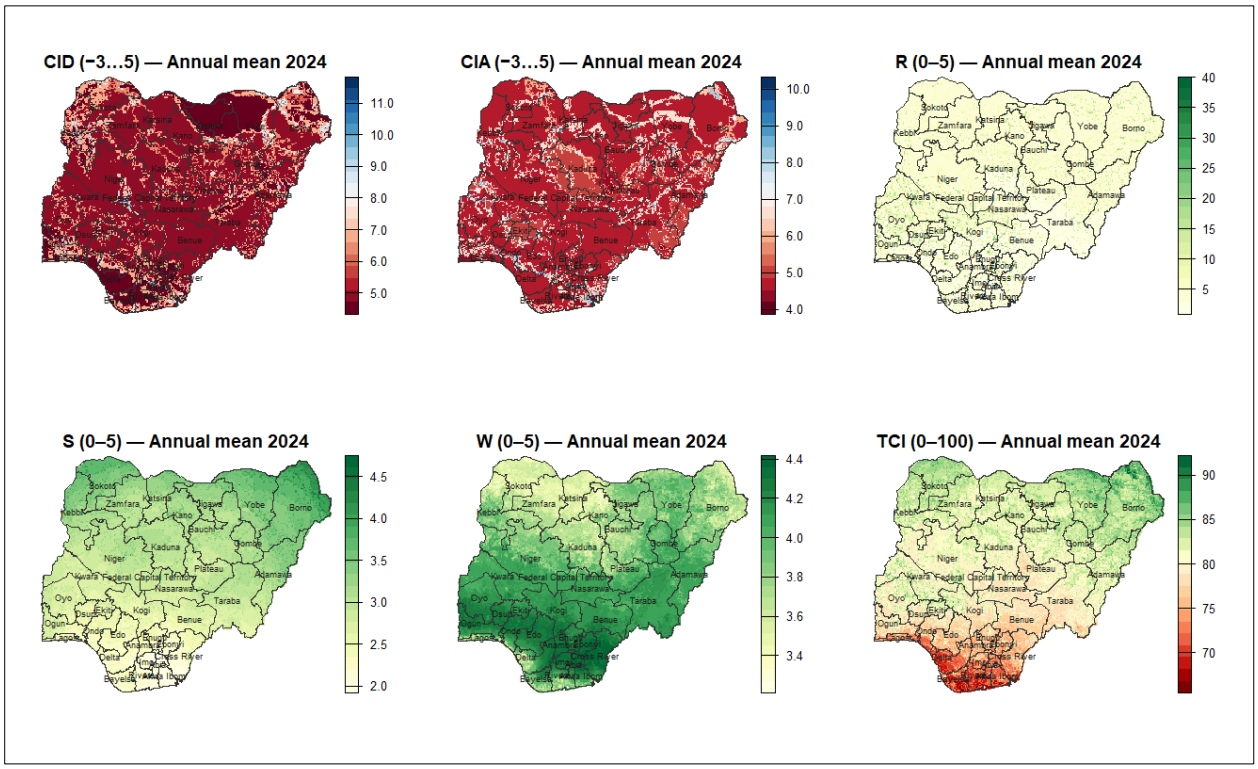

Figure 5. Spatial distribution of tourism climate components and composite index across Nigeria (annual means, 2024).

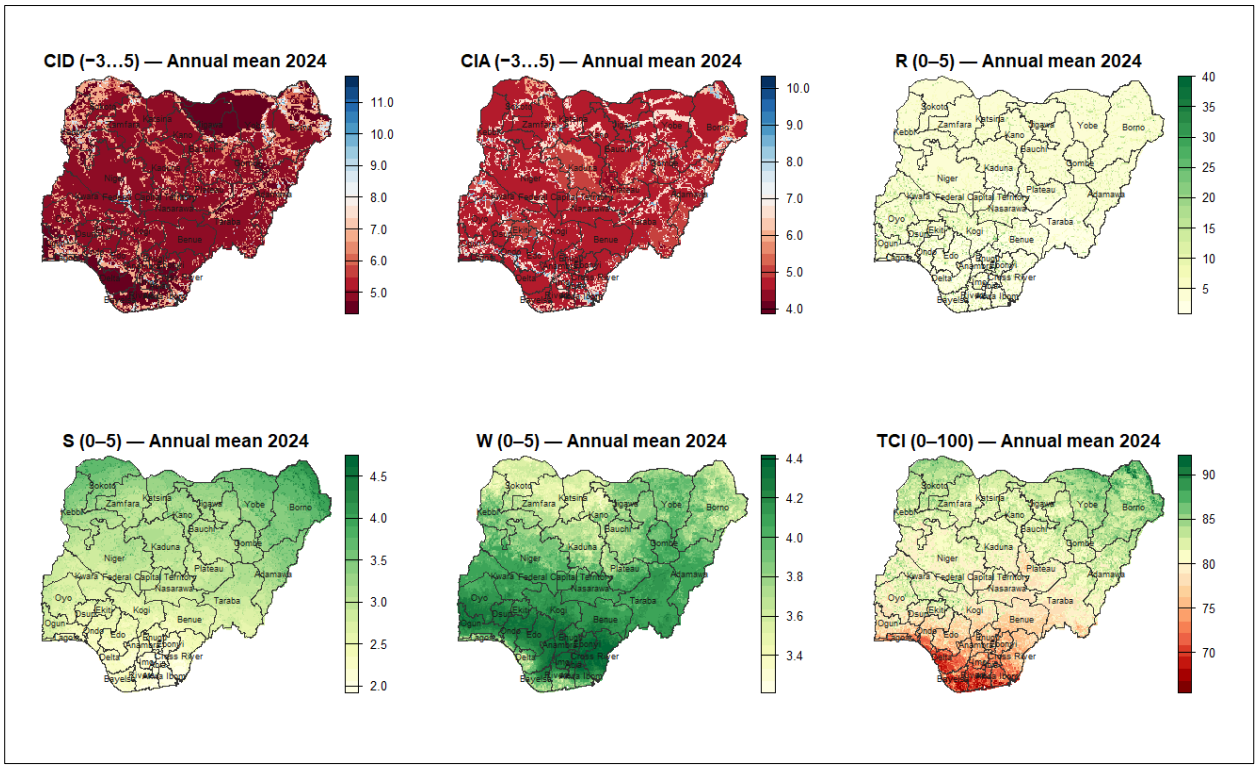

Figure 5 Spatial patterns of tourism climate components and composite index across Nigeria (annual means, 2024)..

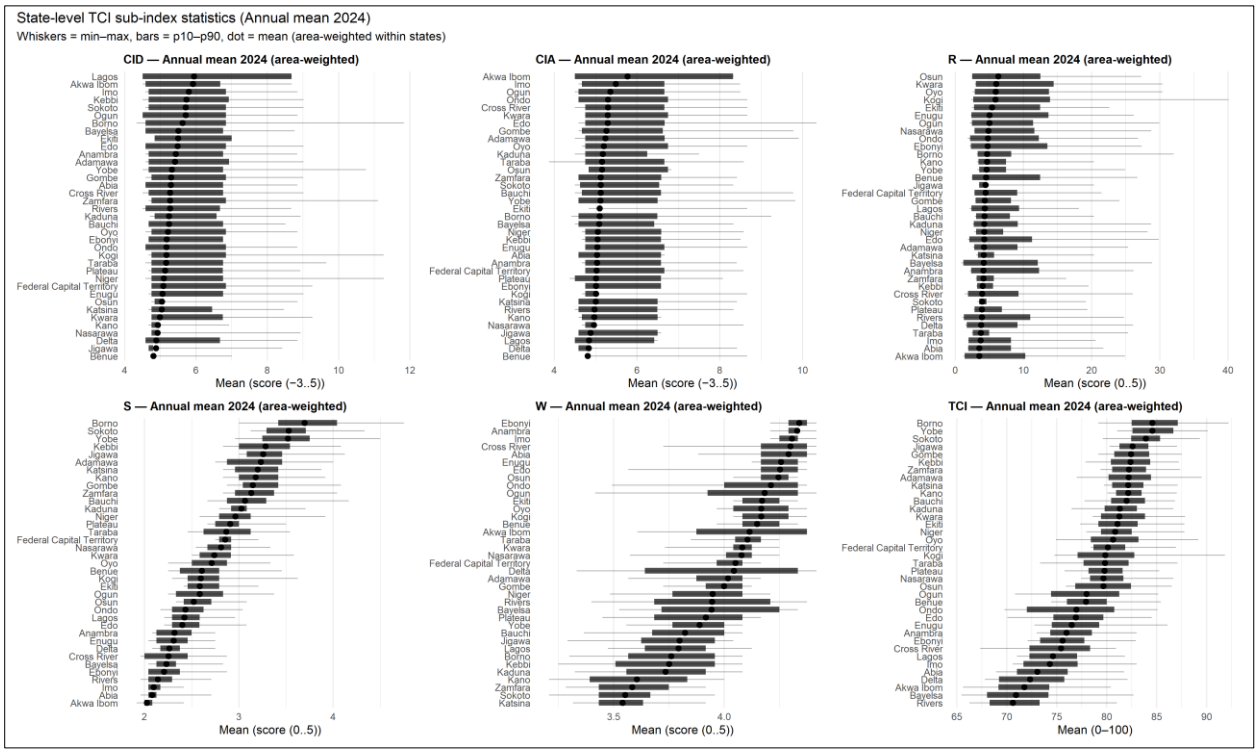

Figure 6. State-level Tourism Climate Index (TCI) sub-index statistics for Nigeria (annual means, 2024).

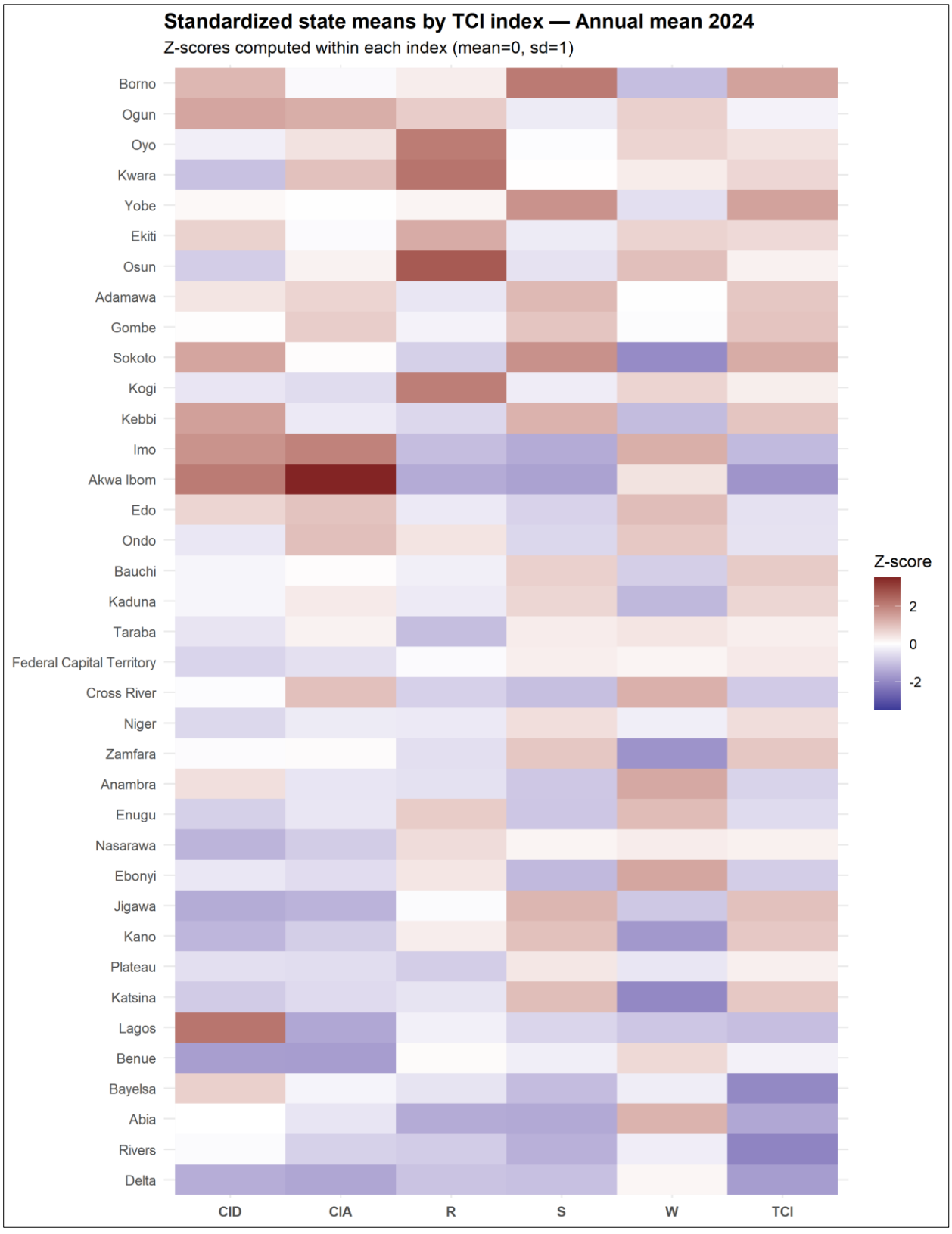

Figure 7. Standardized state-level means of Tourism Climate Index (TCI) components across Nigeria (annual means, 2024).

4. Discussion

4.1 Spatial Patterns and Mechanisms

Our nationwide analysis reveals a coherent, process-based geography of tourism-climate suitability across Nigeria. The semi-arid north and northeast (e.g., Yobe, Sokoto, Jigawa, Gombe) attain the highest Tourism Climate Index (TCI) means, reflecting higher sunshine frequency (S) and reduced rainfall penalties (R), with daytime and 24-h comfort (CID/CIA) near Mieczkowski's "comfort pivot." In contrast, humid coastal states (Rivers, Bayelsa, Akwa Ibom, Delta, Abia, Lagos) show lower scores due to persistent cloudiness, rainfall, and vapor-pressure-driven thermal discomfort (Scott et al., 2016; de Freitas et al., 2017). Orographic and transition-zone states (Plateau, Taraba) exhibit the widest dispersion, consistent with topographic control on temperature, clouds, and wind exposure (Balogun et al., 2016; Akinsanola et al., 2017). The national TCI mosaic aligns with Nigeria's latitudinal hydro-radiative gradient and the West African Monsoon framework (Nicholson, 2013).

4.2 Seasonality and Intra-Annual Range

While state-level TCI standard deviations are modest (≈ 1–3 units), p10–p90 spreads in coastal and interior-southern states reveal pronounced seasonality, driven by monsoonal rainfall and cloud regimes. Northern states display tighter distributions and fewer extreme wet months, yielding more consistent tourism comfort through the year (Sanogo et al., 2015). This spatio-temporal asymmetry supports calendar-aware destination management, where emphasis shifts northward during wet months and toward coastal states in drier periods (Amelung et al., 2007; Gössling et al., 2012).

4.3 Interpreting CID/CIA with the THI Proxy

Mapping Temperature–Humidity Index (THI) to Mieczkowski's CID/CIA categories reproduces the essential heat-humidity interactions that shape perceived comfort in tropical climates (Epstein & Moran, 2006; Rutty & Scott, 2010). THI captures coastal sultriness where moderate Tmax combines with high RH, but it omits direct radiative load, clothing, and metabolic factors (Blazejczyk et al., 2012). During Harmattan months, drier air and clearer skies can raise shortwave flux yet increase perceived comfort—a nuance partially represented through S and W sub-indices. Nonetheless, coupling THI with explicit sunshine, rainfall, and wind metrics preserves the main biophysical trade-offs that underpin tourism suitability in West African climates (Dubois et al., 2016).

4.4 Implications for Tourism Planning and Climate Services

The gridded TCI outputs translate directly into decision support for tourism and recreation management. Seasonal windows with higher composite scores can guide event scheduling, festival planning, and outdoor sports (Scott & Lemieux, 2010). Marketing strategies can align with regional strengths: northern circuits emphasizing clear skies and desert-savanna aesthetics, and coastal experiences framed around short sunshine windows moderated by sea breezes. Integration of TCI calendars with health advisories—heat alerts, hydration guidance, and shaded-infrastructure planning—can mitigate climate-related risks while preserving visitor experience (Perch-Nielsen et al., 2010; UN WTO, 2022).

4.5 Context within Prior Evidence

Observed spatial gradients are consistent with West African Monsoon climatology, characterized by a northward increase in insolation and a southward rise in humidity and rainfall (Nicholson, 2013; Tsanakas et al., 2019). The comfort penalty of humidity and the beneficial effect of moderate wind correspond with previous tropical tourism-climate studies (Cavallaro et al., 2019). Our high-resolution, state-resolved results extend that evidence using a reproducible Earth-Engine–R workflow, yielding administrative summaries tailored to Nigeria's policy and market systems. Elevated

variability across escarpments and highlands further supports earlier findings that topographic micro-climates influence eco-tourism siting and outdoor recreation potential (De Silva et al., 2020).

4.6 Limitations and Uncertainties

Several methodological choices introduce uncertainty. (i) The THI proxy simplifies human energy balance relative to PET or UTCI formulations (Blazejczyk et al., 2012); future work should recalibrate CID/CIA thresholds for tropical conditions. (ii) The Ångström–Prescott coefficients (a, b = 0.25, 0.50) are generic; regional calibration using sunshine records could improve coastal S estimates (Prescott, 1940). (iii) TerraClimate's ~4 km resolution under-represents urban heat islands and coastal complexity (Abatzoglou et al., 2018). (iv) Wind at 10 m may not reflect pedestrian-level exposure; incorporating land-use–based roughness corrections would refine W (Hanna & Chang, 2012). (v) ADM1-level aggregation may mask local heterogeneity; finer reporting at parks or coastal segments is recommended.

4.7 Robustness Checks and Future Directions

Future sensitivity tests should (a) vary THI–CID/CIA mappings and evaluate their effect on composite TCI, (b) re-parameterize R, S, W scoring thresholds for Nigerian market tolerances, and (c) compare alternative comfort indices such as UTCI and PET for representative cities (Bröde et al., 2012). Extending the time series with near-real-time TerraClimate updates would enable early-warning systems for heat or extreme rainfall events. Finally, linking TCI trajectories with mobility, booking, and visitation datasets could quantify elasticity—how tourism demand shifts with climate suitability—supporting adaptive portfolio optimization across Nigeria's states (Gössling et al., 2012; Scott et al., 2019).

5. Conclusions

We produced a reproducible, Nigeria-wide assessment of tourism climate suitability (1991–2024) by converting TerraClimate inputs into FAO-56 intermediates, THI-based comfort (CID/CIA), and the composite TCI. Results show a clear hydro-radiative dipole: **northern states** achieve **higher, more consistent TCI** (more sunshine, less rain), while **humid coastal states** score lower due to cloudiness, rainfall, and high vapor pressure despite milder temperatures; highlands (Plateau, Taraba) are most variable. These state-level, month-by-month metrics can directly guide event timing, destination marketing, and risk management. Key limitations (THI proxy, coastal sunshine calibration, ~4–5 km resolution, 10 m wind exposure) point to next steps—testing UTCI/PET, refining Ångström coefficients, using higher-resolution forcings, and validating with visitation data for operational climate services.

Data availability statement: The satellite data used in this study are open to access as follows:

Landsat: https://developers.google.com/earth-engine/datasets/catalog/landsat,

DEM: https://developers.google.com/earth-engine/datasets/catalog/COPERNICUS_DEM_GLO30

Climate: https://www.climatologylab.org/terraclimate.html

Landcover classes: https://www.esa-landcover-cci.org/

Watershed: https://www.hydrosheds.org/

Author Contributions: Conceptualization, Z.I. and Y.J.C.; methodology, Z.I. F.M. and U.U.E.; formal analysis, Z.I., Y.J.C., and R.K.H.; investigation, U.U.E., Y.J.D., F.M. and R.K.H.; data curation, U.U.E. and E.L.E.; writing original draft preparation, Z.I. and Y.J.C.; writing—review and editing, U.U.E., E.L.E., and R.K.H.; supervision, Z.I.; project administration, Z.I. F.M.and Y.J.C. All authors have read and agreed to the published version of the manuscript.

Funding

This research received no external funding.

Informed Consent Statement

Not applicable.

Data Availability Statement

The data presented in this study are available from the corresponding author upon reasonable request.

Conflicts of Interest

The authors declare no conflict of interest.

Abbreviation

TCI — Tourism Climate Index (0–100; Mieczkowski)

CID — Daytime Comfort Index (TCI thermal component)

CIA — 24-h Comfort Index (TCI thermal component)

THI — Temperature–Humidity Index (thermal comfort proxy)

PPT — Precipitation ($mm \cdot month^{-1}$)

SunH — Sunshine Hours ($h \cdot day^{-1}$)

SRAD — Surface Downwelling Shortwave Radiation ($W \cdot m^{-2}$)

Rs — Daily Global Radiation ($MJ \cdot m^{-2} \cdot day^{-1}$; from SRAD)

WS — Wind Speed at 10 m ($m \cdot s^{-1}$)

VAP — Near-surface Vapor Pressure (kPa)

References

Abatzoglou, J. T., Dobrowski, S. Z., Parks, S. A., & Hegewisch, K. C. (2018). TerraClimate, a high-resolution global dataset of monthly climate and climatic water balance from 1958–2015. *Scientific Data, 5*, 170191. https://doi.org/10.1038/sdata.2017.191

Adedokun, J. A. (1978). West African precipitation and dominant atmospheric mechanisms. *Archives for Meteorology, Geophysics and Bioclimatology Series A, 27*(3), 289–310. https://doi.org/10.1007/BF02248078

Adefisan, E. A., & Abatan, A. A. (2020). Recent climatic trends over Nigeria and implications for sustainable development. *Theoretical and Applied Climatology, 142*(3–4), 1331–1345. https://doi.org/10.1007/s00704-020-03339-8

Akinsanola, A. A., Ogunjobi, K. O., Ajayi, V. O., & Abolude, A. T. (2017). Evaluation of rainfall simulations over West Africa in CMIP5 models. *Theoretical and Applied Climatology, 130*(1–2), 317–332. https://doi.org/10.1007/s00704-016-1888-8

Allen, R. G., Pereira, L. S., Raes, D., & Smith, M. (1998). *Crop Evapotranspiration: Guidelines for Computing Crop Water Requirements (FAO Irrigation and Drainage Paper 56).* FAO. https://doi.org/10.1016/S0378-3774(98)00054-2

Amelung, B., Nicholls, S., & Viner, D. (2007). Implications of global climate change for tourism flows and seasonality. *Journal of Travel Research, 45*(3), 285–296. https://doi.org/10.1177/0047287506295937

Ayuba, H. K., Dami, A., & Amadi, D. C. (2018). Topographic influences on rainfall distribution in central Nigeria. *Nigerian Journal of Environmental Sciences, 12*(1), 15–27.

Balogun, I. A., Yusuf, S. O., & Adedokun, J. A. (2016). Spatial variability of temperature and precipitation trends in Nigeria (1901–2010). *Weather and Climate Extremes, 12*, 24–33. https://doi.org/10.1016/j.wace.2016.02.002

Blazejczyk, K., Broede, P., Fiala, D., Havenith, G., Holmér, I., Jendritzky, G., & Kuchcik, M. (2012). Principles of the Universal Thermal Climate Index (UTCI) and its application. *International Journal of Biometeorology, 56*(3), 431–438. https://doi.org/10.1007/s00484-011-0454-1

Bröde, P., Fiala, D., Blazejczyk, K., Holmér, I., Jendritzky, G., Kampmann, B., ... & Havenith, G. (2012). Deriving the Universal Thermal Climate Index (UTCI). *International Journal of Biometeorology, 56*(3), 481–494. https://doi.org/10.1007/s00484-011-0456-z

Cavallaro, F., Nocera, S., & Preto, A. (2019). Climate change and tourism demand: A review of quantitative studies. *Tourism Management Perspectives, 31*, 287–300. https://doi.org/10.1016/j.tmp.2019.05.005

de Freitas, C. R., Scott, D., & McBoyle, G. (2017). The assessment of climate for tourism: A review of applications and refinements of the Tourism Climate Index. *International Journal of Biometeorology, 61*(12), 1671–1691. https://doi.org/10.1007/s00484-017-1389-3

De Silva, C., Pattiaratchi, C., & Hettiarachchi, S. (2020). Topographic influences on local climate variability and coastal tourism potential. *International Journal of Climatology, 40*(S1), E321–E339. https://doi.org/10.1002/joc.6231

Dubois, G., Scott, D., Ceron, J.-P., & Gössling, S. (2016). Climate change and tourism in developing countries. *Tourism and Hospitality Research, 16*(1), 47–66. https://doi.org/10.1177/1467358415600218

Epstein, Y., & Moran, D. S. (2006). Thermal comfort and the heat stress indices. *Industrial Health, 44*(3), 388–398. https://doi.org/10.2486/indhealth.44.388

Funk, C., Peterson, P., Landsfeld, M., Pedreros, D., Verdin, J., Rowland, J., ... & Michaelsen, J. (2015). The Climate Hazards Infrared Precipitation with Stations (CHIRPS) dataset. *Scientific Data, 2*, 150066. https://doi.org/10.1038/sdata.2015.66

Gorelick, N., Hancher, M., Dixon, M., Ilyushchenko, S., Thau, D., & Moore, R. (2017). Google Earth Engine: Planetary-scale geospatial analysis for everyone. *Remote Sensing of Environment, 202*, 18–27. https://doi.org/10.1016/j.rse.2017.06.031

Gössling, S., Scott, D., Hall, C. M., Ceron, J.-P., & Dubois, G. (2012). Consumer behavior and demand response of tourists to climate change. *Annals of Tourism Research, 39*(1), 36–58. https://doi.org/10.1016/j.annals.2011.11.002

Hanna, S. R., & Chang, J. C. (2012). Setting minimum turbulence levels in air-quality models. *Atmospheric Environment, 46*, 200–212. https://doi.org/10.1016/j.atmosenv.2011.09.036

Hargreaves, G. H., & Samani, Z. A. (1985). Reference crop evapotranspiration from temperature. *Applied Engineering in Agriculture, 1*(2), 96–99. https://doi.org/10.13031/2013.26773

Hijmans, R. J. (2023). *terra: Spatial data analysis.* R package version 1.7-78. https://CRAN.R-project.org/package=terra

Linacre, E. T. (1992). Climate data and resources: A reference and guide. *Routledge.*

Mieczkowski, Z. (1985). The Tourism Climate Index: A method of evaluating world climates for tourism. *Canadian Geographer, 29*(3), 220–233. https://doi.org/10.1111/j.1541-0064.1985.tb00365.x

Mora, C., Dousset, B., Caldwell, I. R., Powell, F. E., Geronimo, R. C., Bielecki, C. R., ... & Trauernicht, C. (2017). Global risk of deadly heat. *Nature Climate Change, 7*(7), 501–506. https://doi.org/10.1038/nclimate3322

National Bureau of Statistics (NBS). (2022). *Demographic Statistics Bulletin 2022.* Abuja, Nigeria.

Niang, I., Ruppel, O. C., Abdrabo, M. A., Essel, A., Lennard, C., Padgham, J., & Urquhart, P. (2014). Africa. In V. R. Barros et al. (Eds.), *Climate Change 2014: Impacts, Adaptation, and Vulnerability* (pp. 1199–1265). Cambridge University Press.

Nicholson, S. E. (2013). The West African Monsoon: Variability and trends. *Annual Review of Earth and Planetary Sciences, 41*, 101–135. https://doi.org/10.1146/annurev-earth-040809-152353

Odjugo, P. A. O. (2011). Regional evidence of climate change in Nigeria. *Journal of Geography and Regional Planning, 4*(6), 142–150. https://doi.org/10.5897/JGRP10.139

Office of the Surveyor-General of the Federation (OSGOF). (2019). *Administrative Boundaries of Nigeria (ADM1–ADM3) Dataset.* Abuja, Nigeria: OSGOF Geospatial Data Centre.

Oguntunde, P. G., Abiodun, B. J., & Lal, R. (2017). Changing temperature, rainfall and extreme climate events in Nigeria, 1981–2010. *International Journal of Climatology, 37*(Suppl 1), S32–S46. https://doi.org/10.1002/joc.5028

Oladipo, E. O. (1995). Some aspects of the spatial characteristics of drought in northern Nigeria. *Natural Hazards, 12*(2), 171–188. https://doi.org/10.1007/BF00593359

Olaniran, J. A., Akinsanola, A. A., & Adefisan, E. A. (2020). Understanding Nigeria's climatic zones in relation to rainfall variability and temperature extremes. *Atmospheric Research, 239*, 104897. https://doi.org/10.1016/j.atmosres.2020.104897

Omotosho, J. B. (2008). Precipitation and climate variability in Nigeria during the 20th century. *Theoretical and Applied Climatology, 92*(1–2), 93–102. https://doi.org/10.1007/s00704-007-0312-5

Perch-Nielsen, S. L., Amelung, B., & Knox, J. A. (2010). The vulnerability of beach tourism to climate change—An index approach. *Climatic Change, 100*(3–4), 579–606. https://doi.org/10.1007/s10584-009-9687-9

Perch-Nielsen, S. L., Amelung, B., & Knox, J. A. (2010). The vulnerability of beach tourism to climate change—An index approach. *Climatic Change, 100*(3–4), 579–606. https://doi.org/10.1007/s10584-009-9687-9

Prescott, J. A. (1940). Evaporation from a water surface in relation to solar radiation. *Transactions of the Royal Society of South Australia, 64*, 114–118.

Rutty, M., & Scott, D. (2010). Will the Mediterranean become 'too hot' for tourism? *A reassessment using the Tourism Climate Index. Climatic Change, 105*(3–4), 427–436. https://doi.org/10.1007/s10584-010-9815-x

Sanogo, S., Fink, A. H., Omotosho, J. B., Ba, A., Redl, R., & Zoungrana, E. (2015). Spatio-temporal characteristics of the recent rainfall recovery in West Africa. *International Journal of Climatology, 35*(15), 4589–4605. https://doi.org/10.1002/joc.4309

Scott, D., & Lemieux, C. J. (2010). Weather and climate information for tourism. *Procedia Environmental Sciences, 1*, 146–183. https://doi.org/10.1016/j.proenv.2010.09.011

Scott, D., de Freitas, C. R., & Mieczkowski, Z. (2016). Assessing tourism-climate relationships: Quantifying the biophysical and perceived suitability of climates for tourism. *Tourism Management, 52*, 506–517. https://doi.org/10.1016/j.tourman.2015.06.018

Scott, D., Hall, C. M., & Gössling, S. (2019). Global tourism vulnerability to climate change. *Annals of Tourism Research, 77*, 49–61. https://doi.org/10.1016/j.annals.2019.05.007

Scott, D., Hall, C. M., & Gößling, S. (2019). Global tourism vulnerability to climate change. *Annals of Tourism Research, 77*, 49–61. https://doi.org/10.1016/j.annals.2019.05.007

Tsanakas, K., Houssos, E. E., Lolis, C. J., & Feidas, H. (2019). Rainfall seasonality and variability over West Africa in recent decades. *Atmospheric Research, 227*, 240–252. https://doi.org/10.1016/j.atmosres.2019.05.007

United Nations Department of Economic and Social Affairs (UNDESA). (2023). *World Population Prospects 2022: Summary of Results.* New York: United Nations.

United Nations World Tourism Organization (UN WTO). (2022). *Tourism and Climate Action: Policy Guidelines for a Resilient Sector.* Madrid: UN WTO. https://doi.org/10.18111/9789284423288

World Bank. (2023). *Nigeria Urbanization Review: Pathways to Sustainable Urban Growth.* Washington, DC: World Bank Group. https://doi.org/10.1596/978-1-4648-1942-1